Measuring absorption coefficients in small volumes of highly scattering media: source-detector separations for which path lengths do not depend on scattering properties

Judith R. Mourant, Irving J. Bigio, Darren A. Jack, Tamara M. Johnson, and Heather D. Miller

The noninvasive measurement of variations in absorption that are due to changes in concentrations of biochemically relevant compounds in tissue is important in many clinical settings. One problem with such measurements is that the path length traveled by the collected light through the tissue depends on the scattering properties of the tissue. We demonstrate, using both Monte Carlo simulations and experimental measurements, that for an appropriate separation between light-delivery and light-collection fibers the path length of the collected photons does not depend on scattering parameters for the range of parameters typically found in tissue. This is important for developing rapid, noninvasive, and inexpensive methods for measuring absorption changes in tissue. © 1997 Optical Society of America

Key words: Absorbance measurements, turbid media, tissue absorption, concentration measurements.

1. Introduction

Noninvasive, *in vivo* methods for measuring absorption coefficients of tissue are potentially very useful biomedical tools. Applications include measurements of endogenous compounds such as hemoglobin, bilirubin, and cytochrome oxidase, as well as determining concentrations of exogenous chromophores such as photodynamic therapy and chemotherapy drugs. The specific case of chemotherapy drugs can be used to illustrate the potential benefits of a noninvasive or minimally invasive method for measuring local tissue concentrations. The therapeutic benefit of chemotherapy drugs is determined by the tissue concentration of the drug in the targeted site. The only minimally invasive check available to the oncologist is to track the blood-serum concentration and assume a relationship to the tissue concentration.[1] This assumption is unreliable.[2] Other methods for tracking pharmicokinetics locally, such as microdialysis, are invasive.[3] The ability to track compound concentrations by examining a change in absorption that is due to the presence of the drug in tissue noninvasively would be a tremendous advantage in clinical pharmacology, especially for the development of new drugs.[4]

Most work to date has concentrated on making optical measurements in a geometry for which the diffusion approximation is applicable,[5–8] although neural-network analysis methods have also been used.[9,10] In this paper we describe a method for measuring small absorption changes by means of a backscattering geometry for which the diffusion approximation is not valid. Rather than a frequency domain or time resolved approach, a simpler and consequently less expensive steady-state method is applied. A further advantage of making steady-state measurements is that a wavelength range greater than 500 nm can be measured in less than 1 s.

The underlying idea in this paper is that, when light delivery and collection are performed with fiber optics in contact with the tissue surface, there is an optimum separation between the source and the detector fibers for which the dependence of the path length on scattering parameters is minimal. This idea can arise from examination of the path lengths

The authors are with Bioscience and Biotechnology Group CST-4, MS E535, Los Alamos National Laboratory, Los Alamos, New Mexico 87545.

Received 27 September 1996; revised manuscript received 23 December 1996.

0003-6935/97/225655-07$10.00/0

for very small and very large source–detector separations. In general, for very small fiber separations, the average path length of the collected photons is longer for a less-scattering media with higher g values than for a highly scattering media with lower g values because the photons need to undergo a certain number of high-angle scattering events to nearly reverse their direction of travel.[11] At very large fiber separations one expects the path length to be longer for the more highly scattering media, as is obvious in the case of light transmission. Therefore there must be some crossover regime in the middle for which the average path lengths for different scattering media are quite similar.

The first part of the approach taken in developing this method was to investigate general characteristics of light-scattering measurements at small fiber separations using Monte Carlo simulations. Based on general trends observed in the Monte Carlo simulations measurement techniques were then developed by experimentation on tissue phantoms.

2. General Principles

Knowledge of the path length L traveled by collected photons permits the use of Beer's law, given in Eq. (1), where I is the collected light, μ_a is the absorption coefficient of the medium, and I_o is the incident light intensity:

$$I = I_o \exp(-\mu_a L). \tag{1}$$

For the purpose of discussion we assume that the path length does not depend on wavelength. Then, by comparing the signals at two different wavelengths, it is possible to determine the difference in absorption coefficients at the two wavelengths:

$$\mu_a(\lambda_1) - \mu_a(\lambda_2) = -\ln\left[\frac{I(\lambda_1)/I_o(\lambda_1)}{I(\lambda_2)/I_o(\lambda_2)}\right]\Big/L. \tag{2}$$

For a chromophore with a sharp absorption band (e.g., absorbing at λ_1 but not λ_2), Eq. (2) should have great utility for measuring changes in the concentration of a chromophore when L is known. We will show below that, for certain source–detector separations, the path length depends only weakly on the scattering properties over the range found in tissue. We also find that small changes in absorption have a negligible effect on path length. Therefore, if the difference in absorption at λ_1 and λ_2 is small (we are only concerned with small changes in absorption) and appropriate fiber separations are chosen, the above assumption that the path length does not depend on wavelength is valid.

3. Monte Carlo Simulations

To investigate characteristics of light scattering with small source–detector separations, we performed Monte Carlo simulations by using a previously described code.[10] Reflection and refraction at interfaces between different media and the numerical aperture of the light-delivery and light-collection fibers are accounted for in the code. Henyey–Greenstein phase functions were used in the simulation, and the effects of different values of $g = \langle \cos\theta \rangle$ were assessed. The delivery and collection fibers were modeled as being 200 μm in diameter with a numerical aperture of 0.34.

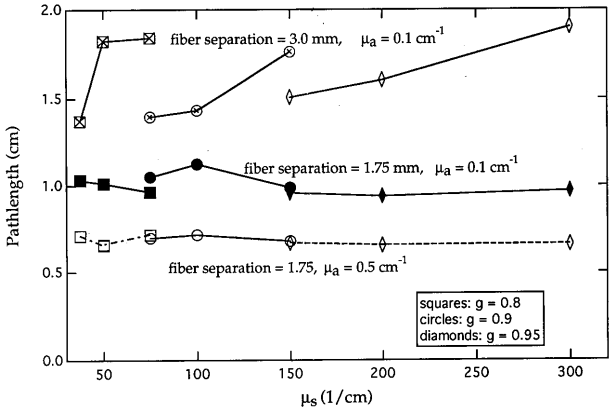

Fig. 1. Average path lengths of photons traveling from a delivery fiber to a collection fiber (in a backscatter geometry such as that shown in Fig. 1) as calculated by Monte Carlo simulations. Results are shown for three sets of source- and detector–fiber center-to-center separations, d, and values of μ_a. For $d = 1.75$ and $\mu_a = 0.5$ cm^{-1} the percent difference in path lengths is 9.5%. For $d = 1.75$ and $\mu_a = 0.1$ cm^{-1} the difference in path lengths is ~16%. For $d = 3.0$ and $\mu_a = 0.1$ cm^{-1} the percent difference in path lengths is 30%. The error bars are smaller than the symbols and were determined by several simulations with different numbers of incident photons. Simulations in which more than 400 photons were collected all resulted in the same value (to within 0.1%) of the path length. Deviations from this value when smaller numbers of photons were collected were used to estimate the errors.

In Fig. 1 the average path length traveled by the collected photons is plotted versus the scattering coefficient, μ_s, of the medium with the anisotropy factor, g, adjusted to keep $\mu_s' = \mu_s(1 - g)$ within the range 7.5–15 cm^{-1}. Results are shown for three sets of source- and detector-fiber center-to-center separations, d, and values of μ_a. For $d = 1.75$ and $\mu_a = 0.5$ cm^{-1} the greatest percent variation in path length for different scattering parameters is 9.5%. This demonstrates that for the correct choice of fiber separation the average path length traveled by the collected photons depends only weakly on scattering characteristics.

Interesting issues with regard to Fig. 1 are (1) whether the essential lack of dependence on scattering properties is valid for the range of absorption parameters found in tissue and (2) whether the choice of fiber separation and the variation in path length depend on properties of the optical delivery and collection system. With regard to the second issue, fiber numerical aperture was found to have a negligible effect on the path length. Path lengths determined from Monte Carlo simulations with numerical apertures of 0.22 and 0.34 agreed within errors for all but two data points for $d = 1.75$ and $\mu_a = 0.5$ cm^{-1}.

The average path lengths of photons traveling from a source to a collection fiber may not be the same in media with the same scattering coefficients but dif-

ferent absorption coefficients. To investigate how this might affect the choice of optimal fiber separation, simulations with the same scattering parameters as in Fig. 1 were performed, but with absorption coefficients of 2.0 cm^{-1} and 0.1 cm^{-1}. For an absorption coefficient of 2 cm^{-1}, it was found that at source–detector separations of 1.25, 1.75, and 2.25 mm the variation in path lengths was 17%, 7%, and 14%, respectively. For an absorption coefficient of 0.1 cm^{-1} there is a 40% variation between the longest and the shortest average path lengths at a separation of 1.0 mm. At fiber separations of 1.5, 1.75 (see Fig. 1), 1.87, and 2.0 mm the variation in path lengths is 16%–20%. When fiber separation is increased to 3.0 mm, the variation in path lengths increases back to ~40% (see Fig. 1). This suggests that there is a range of fiber separations for which the path length is nearly independent of scattering parameters. Furthermore, the choice of optimum source–detector separation may be valid for a range of absorption coefficients. For example, the 1.75-mm separation found to have less than a 10% variation in path length as a function of scattering properties when the absorption coefficient is 0.5 cm^{-1} would also work well for measurements in a medium with an absorption coefficient of 0.1 or 2.0 cm^{-1}.

4. Experimental Methods

A cw xenon arc lamp (Optical Radiation Corporation compact lamp, Azusa, California) was used as a light source. All optical fibers were 200 μm in diameter with a numerical aperture of 0.22 (C Technologies, Verona, New Jersey, part number MM0002). One fiber was used to deliver light to the tissue phantom, and several fibers were used for light collection at different distances from the delivery fiber. The incident light power on the sample was ~1.5 mW. The source–detector separations were 0.7, 0.95, 1.2, 1.42, 1.7, 2.18, 2.4, 2.65, 2.98, and 3.2 mm. Light from eight of the collection fibers was simultaneously dispersed by a spectrograph (Acton Research Corporation, Acton, Massachusetts, spectrometer number 275i) and focused onto a two-dimensional thermoelectrically cooled CCD array (Princeton Instruments, Princeton, New Jersey). In this manner one axis of the CCD array corresponded to wavelength while the other axis corresponded to collection fibers at different distances from the source fiber. Signal integration times were less than or equal to 1 s. To account for any fluctuations in lamp intensity some light from the lamp was attenuated and sent directly to the spectrometer. A schematic of the experimental setup is shown in Fig. 2.

Aqueous suspensions of polystyrene spheres (Duke Scientific Corporation, Palo Alto, California) and Intralipid-10% (Pharmacia, Inc, Clayton, New Jersey) were used as scattering media. Measurements were made in 5%, 10%, and 15% concentrations of Intralipid-10%. Based on our previous measurements of the scattering coefficient of Intralipid-10%, these concentrations correspond to reduced scattering coefficients of 7, 15, and 22 cm^{-1} at 550 nm, and

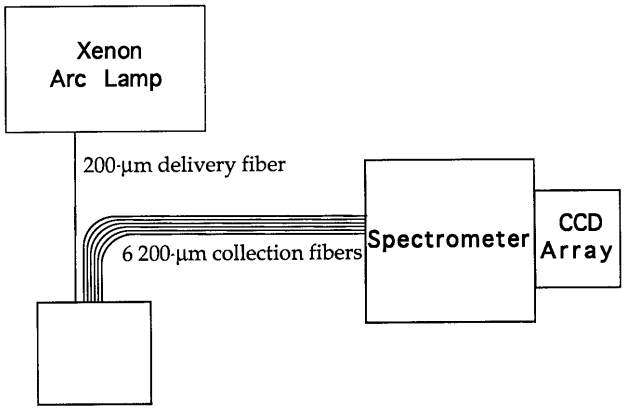

Fig. 2. Schematic of the experimental setup.

reduced scattering coefficients of 5, 10, and 16 cm^{-1} at 650 nm.[12] The value of g at 550 nm is ~0.80, and at 650 nm it is ~0.79.[13] The polystyrene spheres, 0.890 or 0.913 μm in diameter, were used at concentrations of 0.2%, 0.4%, and 0.6% by weight. This corresponds to reduced scattering coefficients of ~7, ~14, and ~21 cm^{-1} at 550 nm, where $g = 0.92$, and reduced scattering coefficients of ~6, ~12, and ~18 cm^{-1} at 650 nm, where $g = 0.91$ as calculated by Mie theory. (An index of refraction of 1.59 was used for the polystyrene spheres.) Fifty milliliters of the suspensions were placed in standard 50-ml beakers and the probe was placed on or near the surface of the suspensions for the measurements. For absorbers, India ink and the dye Direct Blue 71 (Aldrich Chemicals, Milwaukee, Wisconsin, ACS number 4399-55-7) were used. The Direct Blue dye was added to the scattering solutions in aliquots so as to change the absorption coefficient each time by ~0.011 cm^{-1} at 585 nm. Spectra were taken with no Direct Blue dye present and after each addition of Direct Blue dye.

Data were analyzed by division of each spectrum taken with Direct Blue dye present by the spectrum taken before Direct Blue dye was added. The spectra were then normalized to 1 at 800 nm, a wavelength at which Direct Blue dye does not absorb. (This normalization was done because the level of the solution changed during the course of adding blue dye, which slightly changes the total amount of light detected, although it has no measurable effect on the wavelength dependence of collected light.) Finally, the negative natural log was taken over the entire wavelength range. These spectra will be referred to as analyzed spectra, and examples are shown in Fig. 3. The area under the curves from 575 to 595 nm (approximately the peak of the absorption) were then plotted as a function of the absorption coefficient of the added blue dye at 585 nm. Figure 4(a) is an example of such a plot.

The absorbances of the Direct Blue dye and of the India ink in nonscattering, aqueous solutions were measured on a Cary 5E spectrophotometer (Varian Instruments, Sugar Land, Texas) and the spectral shape of the Direct Blue dye was determined to be

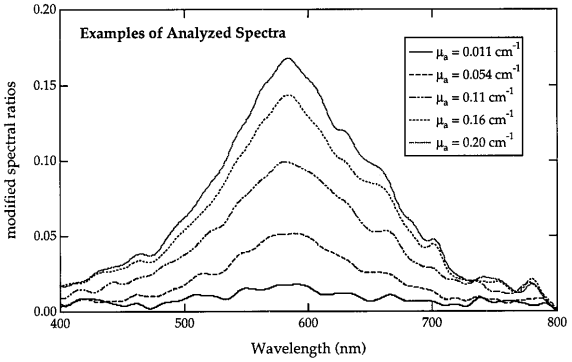

Fig. 3. Spectra taken after the addition of Direct Blue dye, which have been divided by a spectrum with no blue dye, normalized to 1 at 800 nm, and with their negative natural log taken. (The source–detector separation was 1.42 mm. The scattering media was 10% Intralipid-10%.) The values of μ_a given in the figure caption are the average absorption coefficient of the scattering solution from 575 to 595 nm that is due to the addition of the Direct Blue dye.

independent of dye concentration. Spectra of the blue dye and India ink are shown in Fig. 5.

The final part of the experimental investigations was to employ knowledge of the optimum fiber separation for deducing the amount of Direct Blue dye added to a scattering solution. The protocol was as

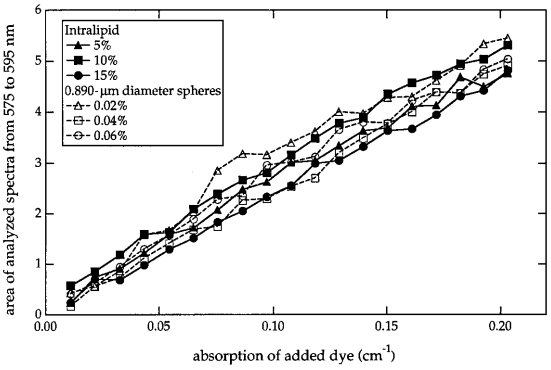

Fig. 4. (a) Areas under the curve from 575 to 595 nm of analyzed spectra plotted versus the average absorption coefficient of the blue dye from 575 to 595 nm; dye was added to the scattering solutions for a source–detector separation of 1.42 mm. (b) Same for a fiber separation of 2.98 mm.

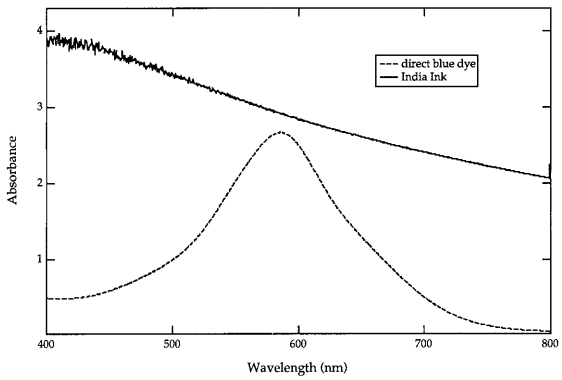

Fig. 5. Absorption spectra of India ink and blue dye.

follows: Measurements of scattering solutions of spheres with India ink were made before and after the addition of aliquots of Direct Blue dye. The data were analyzed without knowledge of the amount of dye that was added.

5. Results

In Fig. 4(a) the areas under the traces of analyzed spectra (see Fig. 3) from 575 to 595 nm are plotted versus the absorption coefficient of the added blue dye at 585 nm for a source-fiber to detector-fiber separation of 1.42 mm. The different curves are for the six different scattering solutions. (India ink was not added to these scattering solutions.) Despite the large range of scattering properties in the different tissue phantoms, the curves in Fig. 4(a) are all very similar. For both larger and smaller fiber separations the slopes of curves like those plotted in Fig. 4(a) depend strongly on scattering properties. This is shown for a fiber separation of 2.98 mm in Fig. 4(b).

To determine the best choice of fiber separation, the percent difference in the area from 575 to 595 nm of the analyzed spectra for the different scattering solutions was plotted versus the fiber separation in Fig. 6. This percent variation in area was calculated according to Eq. (4), where $A_{\min}$ is the minimum value of the area from 575 to 585 nm and $A_{\max}$ is the maximum value of the area from 575 to 595 nm for the set of scattering suspensions measured:

$$\text{percent variation} = \frac{A_{\max} - A_{\min}}{A_{\min}} \times 100. \qquad (3)$$

Values for $A_{\min}$ and $A_{\max}$ were determined by fitting the area curves (e.g., the curves in Fig. 4) to third-order polynomials and use of the values of the fits at an absorbance of 0.15 cm^{-1}. In Fig. 6 the percent variation in the area from 575 to 595 nm of the analyzed spectra are shown for the Intralipid suspensions, for the sphere suspensions, and for the Intralipid and sphere suspensions combined. The percent variation in area is lowest at fiber separations from 1.2 to 1.7 mm.

The effect of the absorption of the starting medium on the optimum choice of source–detector fiber separation was determined. The above measurements on

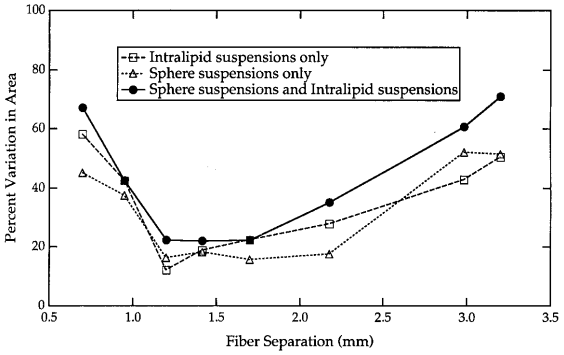

Fig. 6. Percent difference in the largest and smallest areas under the curve from 575 to 595 nm of the analyzed spectra plotted versus the source–detector fiber separation. Analyzed spectra were used for which the amount of added Direct Blue dye had an absorption of 0.15 cm^{-1} at 585 nm. The three scattering suspensions composed of 0.2%, 0.4%, and 0.6% 0.890-μm-diameter spheres had reduced scattering coefficients of ~6, ~12, and ~18 cm^{-1} at 650 nm, where $g = 0.91$. The three scattering suspensions composed of 5%, 10%, and 15% Intralipid-10% had reduced scattering coefficients of 5, 10, and 16 cm^{-1} at 650 nm, where $g = 0.79$.

the three different concentrations of polystyrene spheres were repeated, except that India ink was added to the original solutions to provide a background absorption. The percent difference in the areas from 575 to 595 nm of the analyzed spectra is plotted versus fiber separation in Fig. 7. The percent variation in area is smaller for the data with absorption coefficients of 0.4 and 0.8 cm^{-1} than for the data taken with a background absorption of nearly zero for fiber separations greater than ~1.5 mm.

The final stage of the experimental investigations was to estimate the amount of Direct Blue dye added to a scattering solution. Measurements were made before and after the addition of Direct Blue dye to solutions of spheres to which India ink had been

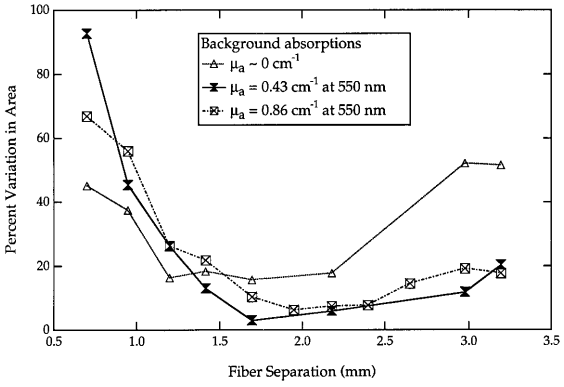

Fig. 7. Percent difference in the largest and the smallest areas under the curve from 575 to 595 nm of the analyzed spectra for the three scattering solutions composed of 0.2%, 0.4%, and 0.6% by weight 0.913-μm-diameter polystyrene spheres plotted versus the source–detector fiber separation. Analyzed spectra were used for which the amount of added Direct Blue dye had an absorption of 0.15 cm^{-1} at 585 nm. Data are given for three different values of μ_a.

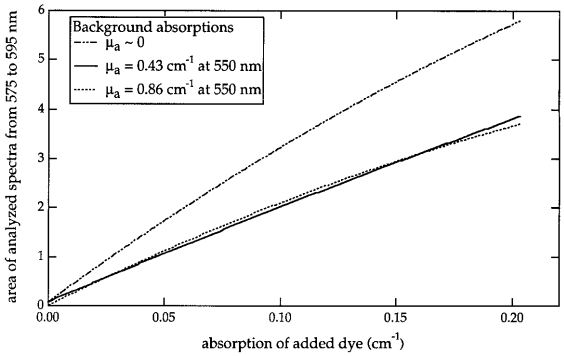

Fig. 8. Best values of the area of analyzed spectra from 575 to 595 nm versus amount of added absorber for a fiber separation of 1.7 mm for three different values of background absorption. These curves were obtained by fitting raw data [similar to that shown in Fig. 4(a)] to a third-order polynomial.

added to yield an absorption coefficient of 0.4 cm^{-1} at 585 nm. The area under the analyzed spectra from 575 to 595 nm for a source–detector separation of 1.7 mm was then computed as before and compared with a calibration curve to determine the change in absorption coefficient. The calibration curve was obtained by fitting of a third-order polynomial simultaneously to the results of earlier measurements taken at a fiber separation of 1.7 mm on three polystyrene sphere suspensions (0.2%, 0.4%, and 0.6% by weight) with a background absorption of 0.4 cm^{-1}. This curve is shown in Fig. 8. The results of the measurements of absorption coefficients are given in Table 1. Differences in the measured and the actual absorption coefficient change varied from 0 to 20%.

6. Discussion

The Monte Carlo and experimental results both indicate that for a particular choice of fiber separation the average path length of the collected photons is quite insensitive to the scattering parameters. The Monte Carlo results show explicitly that the average path length is nearly independent of scattering properties. The experimental results, however, do not directly measure the average path length, $\langle L \rangle$. In a semi-infinite medium there are an infinite number of routes that can be taken from the source to the detector (although very few photons travel some of the routes). Let I_i be the number of photons that start on route i, and let c be any constant. Then

$$-\ln\left(\frac{I}{I_o}\right) = -\ln\left[\frac{\sum_{i=1}^{\infty} I_i \exp(-\mu_a L_i)}{I_o}\right] \neq c\mu_a\langle L\rangle, \quad \sum_{i=1}^{\infty} I_i < I_o. \tag{4}$$

The fact that path length is independent of scattering properties can only be inferred from the experimental data based on the fact that the change in signal due to the addition of an absorber does not depend on scattering properties. Nonetheless, we believe that, on the basis of the experimental and

computational results, it is a good approximation to say that for the correct choice of fiber separation the average path length essentially does not depend on the scattering properties.

For a range of scattering parameters relevant to tissue, and for the optical geometry studied here, the optimal fiber separation was found experimentally to be approximately 1.7 mm for absorption coefficients of 0–0.86 cm^{-1}. This is in reasonable agreement with the Monte Carlo results, which showed that for absorption coefficients of 0.1, 0.5, and 2 cm^{-1} a fiber separation of 1.75 was within the range of optimal fiber separations for each absorption coefficient. For clinical applications the ability to make measurements through an endoscope is advantageous. The source–detector separation of 1.7 mm is less than the diameter of typical endoscope working channels. Therefore endoscopic measurements can take advantage of the fact that at a separation of ~1.7 mm the path length does not depend significantly on the scattering parameters.

What are typical changes in values of absorption coefficients in tissue that are of clinical interest? One area of interest is the measurement of the change in absorption due to the administration of a photodynamic therapy drug. The absorption coefficient of Photofrin in tissue is expected to be roughly 0.01–0.1 cm^{-1} at 630 nm.[14] The technique shown above is therefore applicable to the determination of photodynamic drug therapy concentrations in tissue. Other chromophores of potential interest are hemoglobin and cytochrome oxidase. Based on the expected concentration of cytochrome oxidase in brain tissue and the absorption coefficient of reduced minus oxidized cytochrome,[15] changes in absorption due to changes in the oxygenation of cytochrome oxidase will be approximately 0.003 cm^{-1}. Therefore this technique is probably not applicable to the measurement of changes in the oxidation state of cytochrome oxidase in the brain. This technique is, however, applicable to the measurements of changes in blood oxygenation. Oxyhemoglobin and deoxyhemoglobin have several absorption bands with different molar extinction coefficients. Depending on how much the concentration of hemoglobin changes, an appropriate absorption band can be used to measure the change in concentration. The above is by no means a conclusive list of absorbing compounds of clinical interest. Others include bilirubin, NADH, and chemotherapy drugs. The techniques described in this paper may also be applicable to environmental monitoring and material science applications.

To take advantage of the fact that the path length is independent of the scattering parameters and to use Eq. (2) to determine the absorption coefficient, it is necessary to know the path length or to have a calibration relating the measurement to an absorption coefficient. The curves in Fig. 8 can be used to determine the amount of absorber added to a scattering solution that has a background absorption of either ~0, 0.4, or 0.8 cm^{-1}. This approach was tested for $\mu_a = 0.4$ cm^{-1}, and the results are presented in Table 1. In all cases the errors in the measured change in absorption were less than 20%.

Table 1. Results of Measurements of Absorption Changes due to the Addition of Direct Blue Dye

Solution Type (% 0.913 mm spheres)	Measured Change in Absorbance (cm^{-1})	Actual Change in Absorbance (cm^{-1})	Error (%)
0.2	0.027	0.033	18
0.2	0.070	0.076	7.9
0.4	0.018	0.022	18
0.4	0.077	0.065	18
0.6	0.128	0.108	19
0.6	0.152	0.129	18

The curves for background absorption coefficients of $\mu_a \sim 0$ and $\mu_a = 0.4$ cm^{-1} in Fig. 8 are different from each other, although the curves for $\mu_a = 0.4$ cm^{-1} and $\mu_a = 0.8$ cm^{-1} are very similar. This can be understood by examining the results in Fig. 9, in which the area of analyzed spectra from 575 to 595 nm is plotted against the absorption coefficient of added Direct Blue dye (background $\mu_a \sim 0$). The first part of this curve is steepest, consistent with the trace for $\mu_a \sim 0$ having the steepest slope of the traces in Fig. 8. For values of μ_a greater than 0.4 cm^{-1} the slope of the curve in Fig. 9 does not change very much, and this slope is smaller than the initial slope. Similarly, in Fig. 8 the slopes of the curves for background $\mu_a = 0.4$ cm^{-1} and $\mu_a = 0.8$ cm^{-1} are very similar, and both are less than that for $\mu_a \sim 0$. (The slope of the curve for $\mu_a > 0.4$ cm^{-1} is what one would expect when adding blue dye starting from an average background absorption of 0.4 cm^{-1} at 585 nm.) The fact that the curves for background $\mu_a \sim 0$ and $\mu_a = 0.4$ cm^{-1} are different means that, to take advantage of the fact that the average path length traveled by collected photons is insensitive to the scattering properties, it is necessary to know approximately the original background absorption. Based on the 20% variation [see Fig. 4(a)] in the areas from 575 to 595 nm of the analyzed spectra, the background

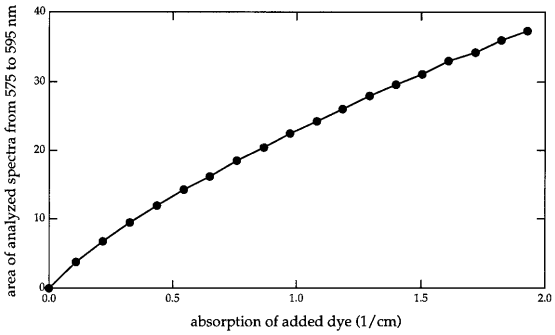

Fig. 9. Areas under the curve from 575 to 595 nm of analyzed spectra plotted versus the average absorption coefficient of the blue dye from 575 to 595 nm; dye was added to the scattering solutions for a source–detector separation of 1.7 mm. The scattering media was 10% Intralipid-10% and the background $\mu_a \sim 0$. The nonlinearity of the curve for small values of μ_a and the linearity of the curve at larger values of μ_a have important consequences for how accurately the background absorbance must be known.

absorption coefficient must be known to an accuracy of $\sim 0.2\ \mathrm{cm}^{-1}$ if it is between 0 and $0.4\ \mathrm{cm}^{-1}$. For larger values of background μ_a, one does not need to know μ_a as accurately, but only to an accuracy of $\sim 2\ \mathrm{cm}^{-1}$, as estimated from Fig. 9. In some cases it may be possible to estimate the background absorption based on *a priori* knowledge of the tissue being measured. For other situations a method for roughly estimating the absorption needs to be developed. Furthermore, if the background absorption varies by more than $0.2\ \mathrm{cm}^{-1}$ across the wavelength range in which the species of interest absorbs, the approximation that the path length is independent of wavelength made in Section 2 becomes invalid.

Finally, it is noted that, although the actual measurements were performed in 50-ml beakers, the actual volume of the scatterer sampled by the light was much smaller. Monte Carlo simulations show that for a fiber separation of 1.48 mm the actual volume interrogated is $\sim 0.1\ \mathrm{cm}^3$ for $g = 0.9$ and $\mu_s = 100\ \mathrm{cm}^{-1}$.

7. Conclusions

We have shown, using both computational methods and experimental data, that with the correct choice of source–detector separation the average photon path length is essentially independent of scattering properties. For the Monte Carlo simulations the tissue-relevant range of parameters investigated was $7.5 < \mu_{s'} < 15\ \mathrm{cm}^{-1}$ with g kept in the range $0.8 < g < 0.95$. In the experimental measurements a larger range of parameters was investigated, with measurements made in suspensions with $\mu_{s'}$ as large as $22\ \mathrm{cm}^{-1}$. The optimum choice of center-to-center separation of the source and the detector fibers was found experimentally to be ~ 1.7 mm. This distance is smaller than the working channel of most endoscopes. Therefore, with a carefully designed probe, it should be possible to take advantage of this effect in endoscopic optical measurements.

To test the utility of the average path lengths being insensitive to scattering parameters, measurements were made of suspensions to which unknown amounts of absorber had been added, and the absolute concentrations of the added absorber were deduced. All the measured values were within 20% of the correct values. This demonstrates the utility of this technique, which does not require the use of a reflectance standard, for measuring small absorption changes.

That the average path length is essentially independent of scattering properties is important for making measurements of small changes in absorption. Possible applications include concentration measurements of NADH, bilirubin, oxyhemoglobin, deoxyhemoglobin, photodynamic therapy drugs, and chemotherapy drugs.

This work was funded by the Laboratory Directed Research and Development program at Los Alamos National Laboratory. Support for Darren A. Jack and Heather D. Miller through the Science and Engineering Research Semester Program sponsored by the Department of Energy is gratefully acknowledged. The authors also acknowledge useful conversations with Bruce J. Tromberg and Andreas H. Hielscher and assistance with the Monte Carlo simulations from James Boyer.

References

1. J. L. Pujol, D. Cupissol, C. Gestinboyer, J. Bres, B. Serrou, and F. B. Michel, "Tumor-tissue and plasma concentrations of platinum during chemotherapy of non-small-cell lung cancer patients," Cancer Chemother. Pharmacol. **27,** 72–75 (1990).
2. M. G. Donelli, M. Zucchetti, and M. Dincalci, "Do anticancer agents reach the tumor target in the human brain?" Cancer Chemother. Pharmacol. **30,** 251–260 (1992).
3. L. Stahle, "Microdialysis in pharmocokinetics," Eur. J. Drug Metab. Pharmokinet. **18,** 89–96 (1993).
4. D. J. Kerr and G. Los, "Pharmacokinetic principles of locoregional chemotherapy," Cancer Surv. **17,** 105–122 (1993).
5. S. Fantini, M. A. Francescini, J. B. Fishkin, and B. Barbieri, "Quantitative determination of the absorption spectra of chromophores in strongly scattering media: a light-emitting-diode based technique," Appl. Opt. **33,** 5204–5213 (1994).
6. B. W. Pogue and M. S. Patterson, "Frequency-domain optical absorption spectroscopy of finite tissue volumes using diffusion theory," Phys. Med. Biol. **39,** 1157–1180 (1994).
7. B. C. Wilson, "Measurement of tissue optical properties: methods and theories," in *Optical-Thermal Response of Laser-Irradiated Tissue*, A. J. Welch and M. J. C. van Gemert, eds. (Plenum, New York, 1995), pp. 233–274.
8. T. J. Farrell and M. S. Patterson, "A diffusion theory model of spatially resolved steady-state diffuse reflectance for the noninvasive determination of tissue optical properties *in vivo*," Med. Phys. **19,** 879–888 (1992).
9. A. Kienle, L. Ligle, M. S. Patterson, R. Hibst, R. Steiner, and B. C. Wilson, "Spatially resolved absolute diffuse reflectance measurements for noninvasive determination of the optical scattering and absorption coefficients of biological tissue," Appl. Opt. **35,** 2304–2314 (1996).
10. P. Marquet, F. Bevilacqua, C. Depeursinge, and E. B. Haller, "Determination of reduced scattering and absorption coefficients by a single charge-coupled-device array measurement, part I: comparison between experiments and simulations," Opt. Eng. **34,** 2055–2063 (1995).
11. J. R. Mourant, J. Boyer, A. H. Hielscher, and I. J. Bigio, "Influence of the scattering phase function on light transport measurements in turbid media performed with small source–detector separations," Opt. Lett. **21,** 546–548 (1996).
12. J. R. Mourant, T. Fuselier, J. Boyer, T. M. Johnson, and I. J. Bigio, "Predictions and measurements of scattering and absorption over broad wavelength ranges in tissue phantoms," Appl. Opt. **36,** 949–957 (1997).
13. H. J. van Staveren, C. J. M. Moes, J. van Marle, S. A. Prahl, and M. J. C. Gemert, "Light scattering in Intralipid-10% in the wavelength range of 400–1100 nm," Appl. Opt. **30,** 4507–4514 (1991).
14. M. S. Patterson, B. C. Wilson, J. W. Feather, D. M. Burns, and W. Pushka, "The measurement of dihemaoporphyrin ether concentration in tissue by reflectance spectrophotometry," Photochem. Photobiol. **46,** 337–343 (1987).
15. C. E. Cooper, S. J. Matcher, J. S. Wyatt, M. Cope, G. C. Brown, E. M. Nemota, and D. P. Delpy, "Near-infrared spectroscopy of the brain: relevance to cytochrome oxidase bioenergetics," Biochem. Soc. Trans. **22,** 974–980 (1994).